Use of 3d-impurity-ion absorption to study the distribution of radiation damage in crystals*

S. I. Yun,[†] K. H. Lee, W. A. Sibley, and W. E. Vehse[‡]

Department of Physics, Oklahoma State University, Stillwater, Oklahoma 74074

(Received 20 February 1974)

The oscillator strengths of spin-forbidden optical transitions of Mn^{2+} are enhanced by the presence of radiation-produced F centers. These enhanced transitions can be used to monitor the presence of other defects in the vicinity of $Mn^{2+}-F$-center complexes. Thus, from absorption and emission changes following irradiation at different temperatures, it appears possible to obtain information on the distribution of radiation-induced interstitials. These data in turn lead to a better understanding of the mechanisms of radiation production and annihilation.

I. INTRODUCTION

In addition to past reasons, the current emphasis on power-production systems such as fast-breeder fission and fusion reactors, which generate copious amounts of radiation and thus create voids and other radiation-damage products in materials,[1] indicates a need for more sensitive techniques to ascertain the distribution of damage products at various temperatures of irradiation. Hobbs *et al.*[2] have made a significant advance using electron microscopy in determining the interstitial cluster distribution in alkali halides after a 300-K irradiation. However, information on the distribution of single interstitials in terms of trapping, migration, etc., is still lacking. This information is particularly important if the focusing mechanism proposed by Silsbee[3] and in more detail by Pooley[4] is a major factor in the total damage process.

Pooley, Hersh, and Lushchik[5,6] have delineated a viable radiation production mechanism for ionic crystals. Pooley further proposed that easy interstitial transfer occurred along close-packed rows of like ions and that this transfer process could result in widely separated vacancy-interstitial pairs. Subsequent work on rutile-structured MgF_2,[7,8] which has no close-packed rows of like ions, suggested that although the transfer process along close-packed directions did not play a significant role in the *production mechanism*, it was important in the *distribution* of the damage products. Thus, in alkali halides, the vacancies and interstitials are expected to be widely separated, whereas in rutile-structured materials they should be close pairs.

Recently,[9-12] it was determined that the presence of an F center (a negative-ion vacancy with a trapped electron) next to a Mn^{2+} substitutional impurity ion increases the absorption by a factor of 100–1000. This increase in oscillator strength for the Mn^{2+} transitions apparently arises from exchange between the defect electron and the Mn^{2+}

electrons. From these results and the normal distribution pattern of $3d$ electrons, it appeared likely that the presence of an interstitial in the vicinity of the $Mn^{2+}-F$-center complex could cause further enhancement of the oscillator strength for some of the transitions and might perturb the energy levels sufficiently that splitting of some of the absorption bands could be observed. The purpose of this paper is to report that low-temperature irradiations of $KMgF_3$ and MgF_2 yield quite different results from 300-K irradiations. This is expected if interstitials are produced as near neighbors and suggests that Mn^{2+} can be used as a sensitive monitor for radiation damage.

II. EXPERIMENTAL

The crystals used in this work were grown by the Stockbarger method or purchased from the Optovac Company. The MgF_2 contained 0.62 at.% and the $KMgF_3$, 1.4 at.% of manganese as deter-
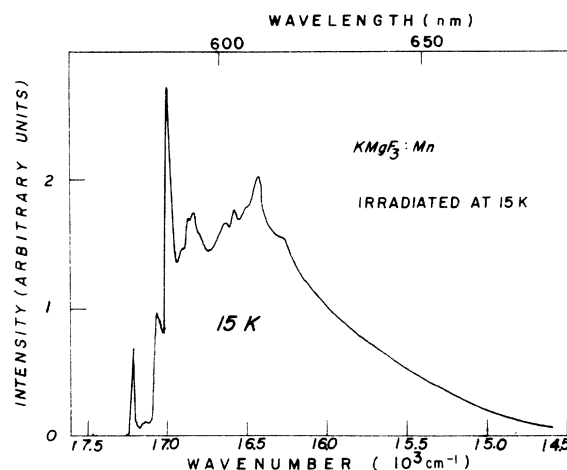

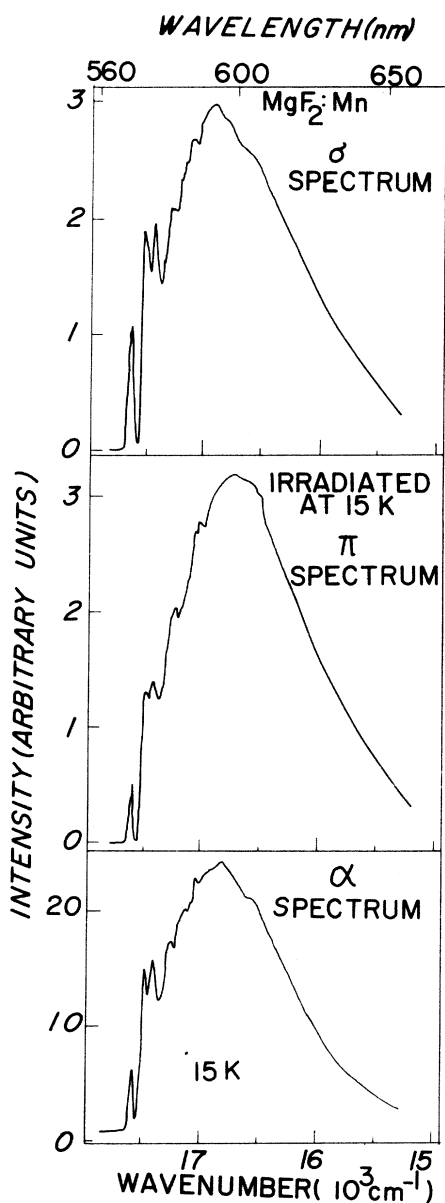FIG. 1. 610-nm emission band present in low-temperature-irradiated or x-ray-stimulated $KMgF_3:Mn$.

FIG. 2. 590-nm emission band observed in low-temperature-irradiated or x-ray-stimulated MgF_2:Mn.

FIG. 3. 680-nm emission band from 15-K electron-irradiated $KMgF_3$:Mn at 15 K.

with a 1-m monochromator and associated electronics as described previously.[9,11] Excitation spectra were taken by setting the 1-m monochromator at the wavelength of the peak of the emission band of interest and then exciting the crystal with light from a Spex 22-cm monochromator. Polarization measurements were made using Glan-Thompson prisms. The excitation source was a 75-W xenon lamp and for this reason the excitation spectra taken between 50 000 and about 35 000 cm^{-1} are not very accurate. A correction for the spectral intensity of the source was made.

III. RESULTS

When $KMgF_3$: Mn is irradiated at any temperature between 15 and 300 K, with even a low dose of high-energy electrons, an emission band with peak at about 610 nm is evident as an afterglow. The same emission band is observed if an unirradiated sample is excited with x rays or a low-temperature irradiated crystal is optically stimulated with 365-

mined by mass spectroscopy. Irradiations were performed with an accelerator using 1.5-meV electrons at a current of 0.2 $\mu A/cm^2$ on the sample. The specimens were cut and polished such that for MgF_2 the c axis was parallel $(c_{\parallel})$ or perpendicular $(c_\perp)$ to the crystal face. The faces of the $KMgF_3$ specimens were {100} planes. The crystals were mounted in a cryogenerator for irradiation and measurement. With the cryogenerator, temperature could be controlled to ±1 K between 15 and 300 K. Optical absorption was measured on a Cary 14 spectrophotometer and emission was detected
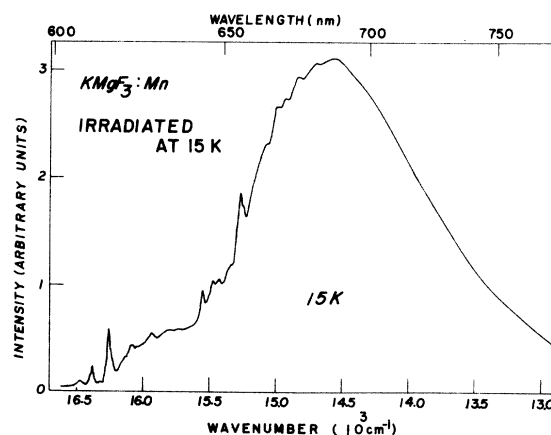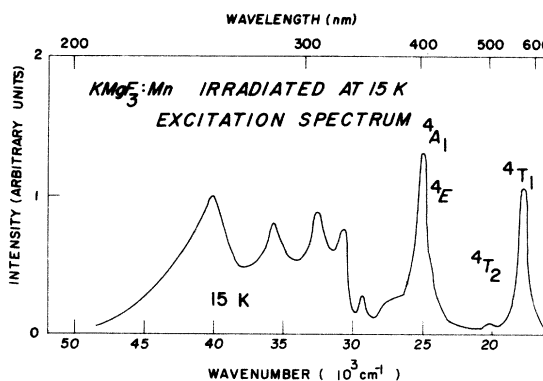

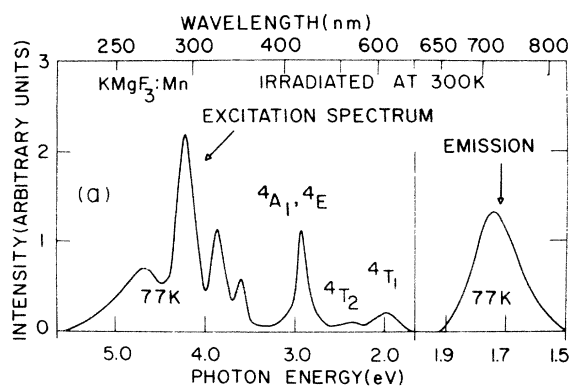FIG. 4. 15-K excitation spectrum for the 680-nm emission in 15-K irradiated $KMgF_3$:Mn.

FIG. 5. 720-nm emission band and 77-K excitation spectra for 300-K electron-irradiated $KMgF_3$: Mn.

nm or 450-nm light. This band is illustrated in Fig. 1. Excitation of unirradiated $KMnF_3$ at 15 K by x rays or optical excitation results in similar emission with slight changes in the sharp line structure. This emission has been attributed in the past to Mn^{2+}.

As shown in Fig. 2, MgF_2 : Mn yields a similar emission band at 590 nm under the same treatments described above. In Fig. 2, the σ, π, and α emission is portrayed. The α spectrum is taken by measuring the unpolarized emission propagating along the c axis of the crystal. The π spectrum is measured with a polarizer oriented such that only the electric vector of the emitted light parallel to the c axis of the crystal ($\vec{E} \parallel \vec{c}$) is transmitted, and the σ spectrum is recorded with the polarizer oriented so that the electric vector perpendicular to the c axis ($\vec{E} \perp \vec{c}$) is passed.

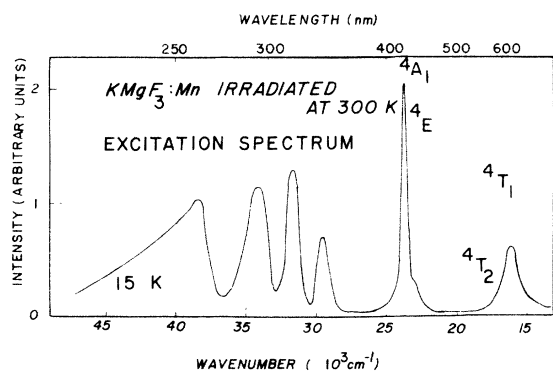After some 20 min in the dark or 1 min under white-light illumination with the sample at 15 K,

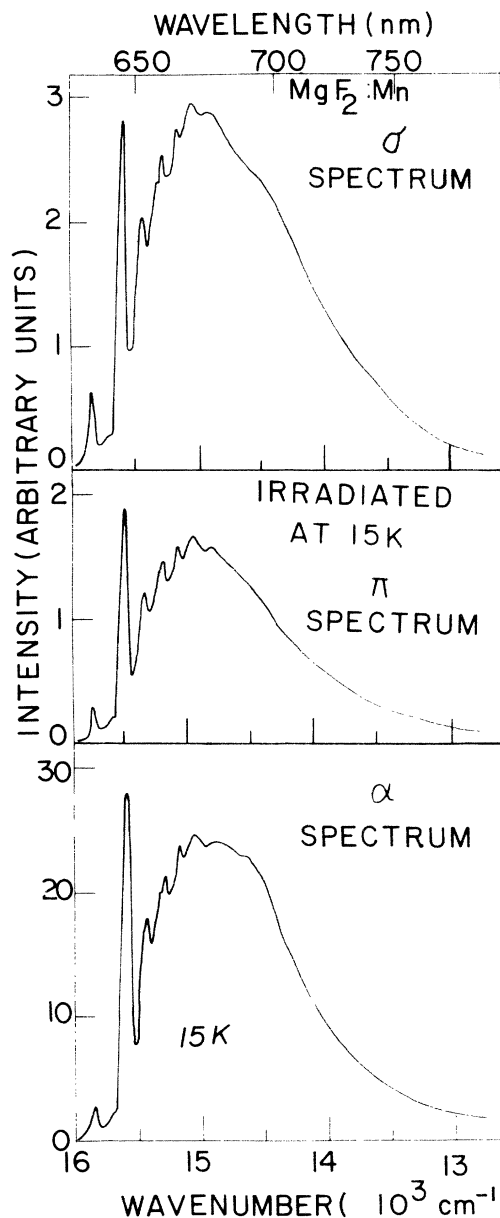FIG. 6. 15-K excitation spectrum for the 720-nm emission band from a 300-K irradiated $KMgF_3$: Mn specimen.

FIG. 7. 670-nm emission band from 15-K electron-irradiated MgF_2 : Mn measured at 15 K.

the emission bands at 610 nm for $KMgF_3$: Mn and 590 nm for MgF_2 : Mn almost disappear. In the case of $KMgF_3$: Mn, when this band has decreased, it is possible to detect emission around 680 nm when measurement is made below 180 K and at 630 nm when the sample is above 180 K. The lifetimes of these bands differ appreciably as has been noted previously.[9] The low-temperature spectrum of this band is shown in Fig. 3, and the excitation spectrum for a sample irradiated and held at 15 K is portrayed in Fig. 4. When $KMgF_3$: Mn crystals which have been irradiated at 15 K and then warmed
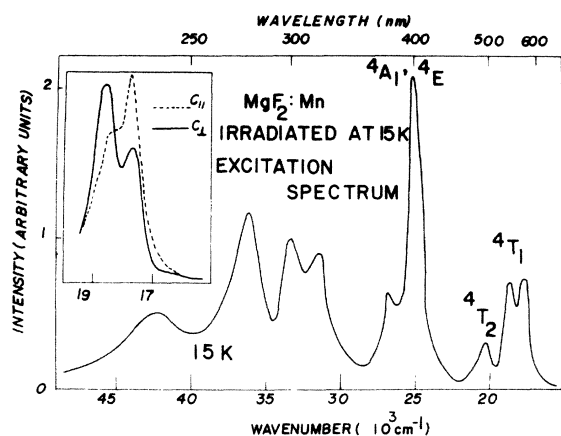
FIG. 8. 15-K excitation spectrum for the 670-nm emission band from a 15-K irradiated MgF_2:Mn crystal. The inset shows the polarized excitation of the $^4T_{1g}$ band.
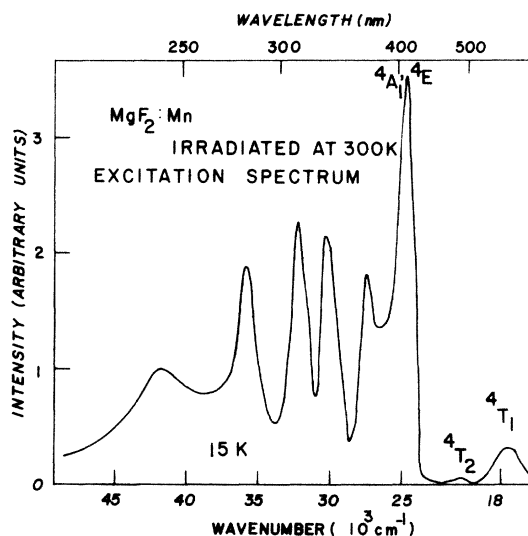
to room temperature are measured at 15 K, the 680-nm band has decreased, but an emission band at 720 nm is present. On the other hand, 300-K irradiated specimens which were measured at low temperature show a 720-nm band but no 680-nm luminescence. The luminescence band at 720 nm and the excitation spectrum for this band taken with the sample at 77 K are shown in Fig. 5. Figure 6 pictures the excitation spectrum with specimen temperature 15 K for the same band.

The σ, π, and α emission spectra for MgF_2: Mn specimens irradiated at 15 K are illustrated in Fig. 7. It should be noted that there is some difference in the intensity of the fine structure between the various spectra. The excitation spectrum for this 670-nm band is shown in Fig. 8. The inset of the figure provides an expanded picture of the $^4T_{1g}$ band at about 570 nm and shows the polarization of the
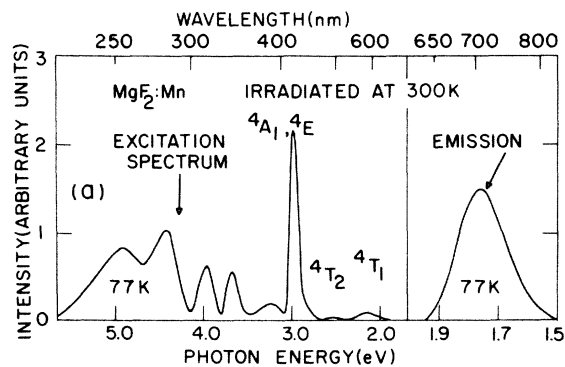

FIG. 9. Excitation spectrum of electron-irradiated MgF_2:Mn measured at 77 K. The emission band that is monitored for the excitation spectrum is shown on the right side of the figure. The crystal orientation is $c_\perp$.

FIG. 10. 15-K excitation for the 700-nm emission band in MgF_2:Mn.

band for the polarizer oriented along the c axis of the crystal ($\vec{E} \parallel \vec{c}$) or perpendicular to the c axis ($\vec{E} \perp \vec{c}$). From the inset it is clear that the two transitions are strongly polarized. Figure 9 shows a 700-nm emission band with its associated excitation spectrum which was taken using a crystal of MgF_2: Mn irradiated at 300 K and measured at 77 K. The defect responsible for these emission and excitation bands evidently does not form during low-temperature irradiation or after low-temperature (either 15 or 77 K) irradiation and warming to 300 K. The 15-K excitation spectrum for the 700-nm band is given in Fig. 10. Although it is not shown clearly in the figure a possible excitation peak occurs at 43 000 cm^{-1}, but because the exciting source is weak in this region the peak is not clearly observed. It should be pointed out that no splitting of the $^4T_{1g}$ excitation peak is observed for the 700-nm emission. The defect responsible for the 670-nm emission forms even during room-temperature irradiation.

Table I indicates the energy differences between the sharp line spectra for the various bands and is presented in such a way that a comparison of $KMgF_3$: Mn and MgF_2: Mn can be made.

Several other experimental observations should be mentioned. No optical absorption or optically stimulated emission bands are observed before irradiation. X-ray excitation with the sample below 50 K does produce a 390-nm emission band in MgF_2: Mn and a 340-nm emission band in $KMgF_3$: Mn. As noted by Kabler[13] and Pooley and Runciman,[14] both of these bands are in the spectral region for X_2^- (V_K) center recombination luminescence, but optical absorption from X_2^- centers in

TABLE I. Phonon lines in $KMgF_3$:Mn and MgF_2:Mn.

KMgF₃:Mn			MgF₂:Mn		
Emission band (nm)	Peak position nm (cm⁻¹)	Energy difference (cm⁻¹)	Emission band (nm)	Peak position nm (cm⁻¹)	Energy difference (cm⁻¹)
				α spectrum	
610	581.0 (17211)	⋯	590	569.0 (17574)	⋯
(excitation	585.8 (17070)	141	(excitation	572.8 (17458)	116
365 nm)	588.7 (16986)	225	365 nm)	575.2 (17385)	189
				579.5 (17256)	318
				π spectrum	
				569.0 (17574)	⋯
				572.5 (17467)	108
				575.0 (17391)	184
				580.8 (17218)	357
				σ spectrum	
				569.2 (17569)	⋯
				573.2 (17446)	123
				575.0 (17391)	178
				580.0 (17241)	328
				α, π, σ spectra	
680	607.4 (16464)	⋯	670	645.7 (15487)	⋯
(excitation	610.1 (16391)	73	(excitation	652.0 (15337)	150
409 nm)	615.0 (16260)	204	540 nm)	658.0 (15198)	289
				663.5 (15072)	415
				669.0 (14947)	540

our doped materials, especially MgF_2, has not been reproducibly observed. X_2^- centers have been studied in other $KMgF_3$ samples.[15,16] When the samples are irradiated at 300 K, F-aggregate centers such as F_2 and F_3 centers can be observed through both emission and absorption spectra. For low-temperature irradiation, no F aggregates are formed. Table II gives a summary of the irradiation observations with a *tentative* identification of

the defects responsible for each emission band.

Immediately after irradiation at temperatures below 80 K, a complicated absorption occurs for $KMgF_3$: Mn and MgF_2 : Mn which decays with time and/or optical bleaching. An optical bleach with 450-nm light decreases the absorption in certain regions rapidly. In Fig. 11, the difference spectra, which are shown as the solid lines, for absorption before and after a 450-nm bleach are de-

TABLE II. Summary of irradiation data; conditions for production of defect.

| Band wavelength (nm) and material	Temp. of observation	e irradiation Low Temp.	e irradiation Low Temp. Warm to Room Temp.	e irradiation Room Temp.	e irradiation X ray, optical Low Temp.	Nature of defect
610; KMgF₃:Mn	15K	⋯	⋯	⋯	Yes-Decays	Mn²⁺ (Unperturbed)
590; MgF₂:Mn	15K	⋯	⋯	⋯	Yes-Decays	Mn²⁺ (Unperturbed)
680; KMgF₃:Mn	15K	Yes	Yes Decreases	No	⋯	Mn²⁺–F-center Interstitial
670; MgF₂:Mn	15K	Yes	Yes Decreases	Yes (Weak)	⋯	Mn²⁺–F-center Interstitial
720; KMgF₃:Mn	15K	No	Yes (Weak)	Yes	⋯	Mn²⁺–F
700; MgF₂:Mn	15K	No	No	Yes	⋯	Mn²⁺–F
340; KMgF₃:Mn	15K	⋯	⋯	⋯	X Ray, Yes	X_2^-(?)
390; MgF₂:Mn	15K	⋯	⋯	⋯	X Ray, Yes	X_2^-(?)
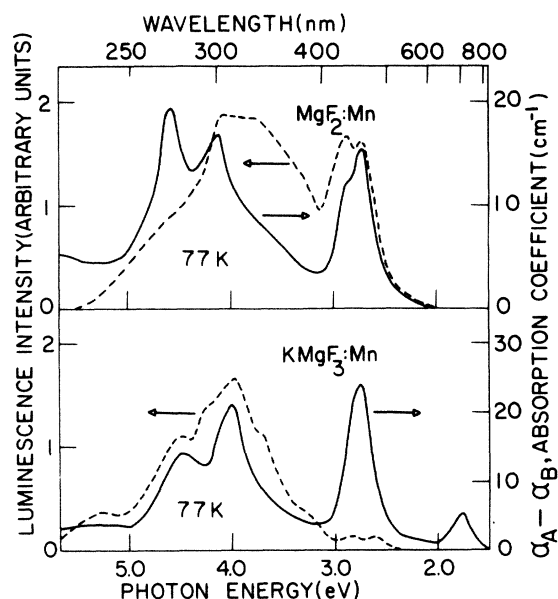
FIG. 11. The dashed lines represent excitation data taken using the 590-nm emission band of MgF_2 : Mn and the 610-nm $KMgF_3$: Mn emission. The solid lines are absorption data taken by subtracting the absorption after irradiation and optical bleaching with 450-nm light, α_B, from the absorption immediately after radiation, α_A.

FIG. 13. Schematic suggestion for the $Mn^{2+}-F$-center-interstitial complex configurations in $KMgF_3$ and MgF_2.

picted. The dashed lines in the figure represent the excitation spectra for the 590- and 610-nm luminescence bands. When optical bleaching is effective and a crystal with cubic structure such as $KMgF_3$ is being used, it is possible to use polarized light to determine the orientation of the defects responsible for the emission and absorption. The data for such a polarized bleach are illustrated in Fig. 12.

IV. DISCUSSION

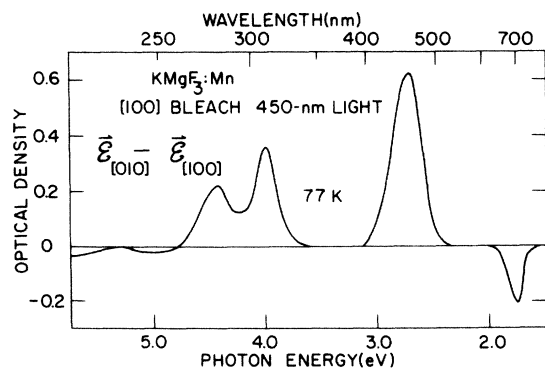In previous work[9-12] the presence of some of the absorption and excitation bands in irradiated

FIG. 12. The difference curve for irradiated $KMgF_3$: Mn bleached with [100]-polarized light.

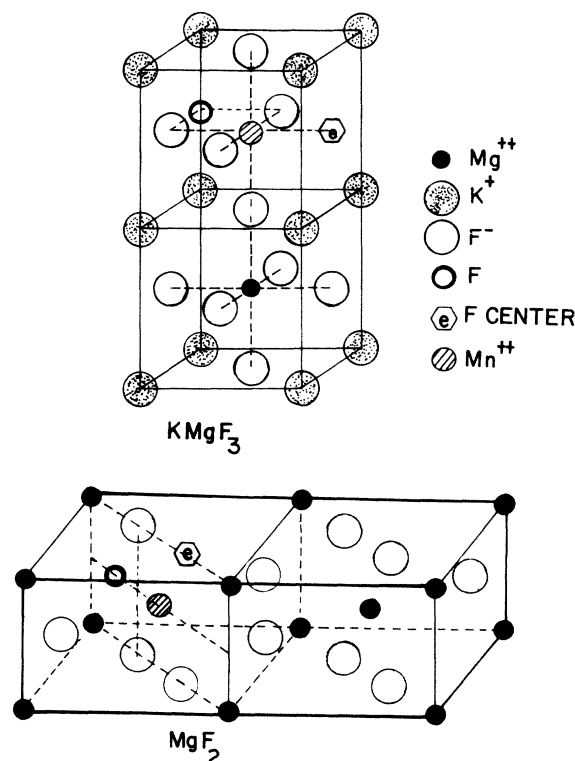MgF_2 : Mn and $KMgF_3$: Mn was attributed to Mn^{2+} ions with F centers as next neighbors. In the past work MgF_2 : Mn was irradiated at room temperature and at this temperature radiation-induced interstitials are mobile and agglomerate. At low temperatures the interstitials should be immobile and other emission and absorption or excitation bands should be observable because of the presence of these defects.

In both $KMgF_3$: Mn and MgF_2 : Mn the emission bands we have studied are different for the different radiation temperatures. The excitation transitions labeled $^4A_1$, ^4E, and $^4T_2$ are enhanced for the low-temperature irradiations compared to the 300-K irradiation. Moreover, for MgF_2, as seen in Fig. 8, it is clear that the $^4T_1$ transition is split. From polarized-light data, shown in the inset of Fig. 8, the dipole direction for the defect responsible for these transitions and the symmetry of the Mn^{2+} defect complex can be found. Previously,[10,11] it was indicated that the 300-K irradiation-induced bands are due to $Mn^{2+}-F$-center defects. Since the low-temperature emission bands and excitation spectra are different, the data are perhaps best explained by assuming that nearby interstitials cause the changes in the optical properties. If this proposal is correct, an analysis of

the polarized-light data in Fig. 8 suggests that the interstitials in 15-K irradiated MgF_2 crystals are located at the center of the triangle connecting the three neighboring Mg ion sites in a {110} plane. The most likely position for interstitial fluorine in $KMgF_3$ is in a {100} plane between four fluorine and two potassium ions. Figure 13 gives a tentative idea of the defect locations in these materials. In the latter structure (perovskite) the possibility of short-range focusing collisions exists, and we might expect an interstitial to be displaced from its vacancy by several lattice spaces even for low-temperature irradiations. Support for this idea comes from the fact that no correlated recombination is observed in $KMgF_3$.[15] As mentioned earlier, at 300 K interstitials are mobile in both materials and aggregate to form clusters. Thus, for 300-K irradiation, the excitation spectra are due only to $Mn^{2+}-F$-center complexes.

For 15- or 77-K irradiation, the emission bands are shifted to shorter wavelengths and are narrower than those induced by a 300-K irradiation. These results suggest that the interstitials push the fluorines neighboring the Mn^{2+} ions in such a way as to give the Mn^{2+} ions more space. When the samples are warmed to room temperature, cooled back to 77 K, and reevaluated, it is found that the emission and excitation spectra from the $Mn^{2+}-F$-center-interstitial complexes are reduced in intensity by a factor of about 50. For 15- or 77-K irradiated MgF_2 no evidence for $Mn^{2+}-F$-center emission is found after warming, and an optical bleach with 254-nm light destroys the defects as does a 300-K electron irradiation.[8] This suggests that only correlated recombination occurs in MgF_2 and the interstitials cannot migrate away except during room-temperature irradiation. For $KMgF_3$: Mn this is not the case. If samples irradiated at 77 K are warmed to 300 K and then recooled to 77 K, both excitation spectra shown in Figs. 4 and 6 are observable; i.e., some of the interstitials jump away instead of recombining with vacancies so that both $Mn^{2+}-F$-center-interstitial and $Mn^{2+}-F$-center complexes are present. This again suggests that in $KMgF_3$ an interstitial is initially further displaced from its vacancy than in MgF_2. No $Mn^{2+}-F$-center-interstitial complexes are present in $KMgF_3$: Mn irradiated at 300 K.

"As-grown" samples and an irradiated sample which was annealed at 800 K for a few hours do not show either 590- or 610-nm luminescence bands during optical excitation. The optically excited emission bands which occur at 590 nm in MgF_2 : Mn and at 610 nm in $KMgF_3$: Mn after irradiation are apparently due to "unperturbed" Mn^{2+} ions, since the emission spectra are essentially the same as observed in MnF_2 and $KMnF_3$. From successive optical-bleaching experiments a linear relation is found between the height of the 450-nm absorption band shown in Figs. 11 and 12 and the 590- or 610-nm luminescence intensity. Furthermore, the afterglow and x-ray-excited luminescence spectra from MgF_2 : Mn and $KMgF_3$: Mn also show 590- or 610-nm bands. The optical-absorption bands for low-temperature irradiated crystals are very complex. Some of the complexity can be reduced by taking difference curves. The difference curves are derived by subtracting the absorption of freshly irradiated crystals. The intensity of the bands and the relationship between the Mn^{2+} emission and the height of the 450-nm absorption suggest that some valence state of manganese is involved. Ikeya and Itoh[17] have done extensive work on Mn^{2+}, Mn^{1+}, Mn^0 in NaCl. Their data suggest that the 450-nm band shown in Figs. 11 and 12 is due to Mn^0 in a substitional site. They ascribe the band at about 270 nm to Mn^{1+}. Our observations are certainly not at variance with their tentative assignments; however, we do feel much work must be done before these suggestions can be substantiated. From our data we feel that Mn^{1+} or Mn^0 centers, with charge compensation from X_2^- centers, are involved.[18,19] This assumption would lead to the possibility of Mn^{2+} emission each time an electron is lost from an Mn^{1+} center as an X_2^- center recombines with Mn^{1+}. However, the $\langle 100 \rangle$ defect symmetry indicated from the polarized optical bleach suggests influence from another nearby defect. The presence of a 700-nm absorption band for $KMgF_3$: Mn and not for MgF_2 : Mn is a mystery.

In summary, the emission bands at 680 nm for $KMgF_3$: Mn and 670 nm for MgF_2 : Mn are due to $Mn^{2+}-F$-center-interstitial complexes, whereas the emission bands at 720 nm for $KMgF_3$: Mn and 700 nm for MgF_2 : Mn are due to $Mn^{2+}-F$-center complexes. Although much work must yet be done to verify the presence and position of interstitial fluorines, we feel that the data presented above make quite evident the great potential of using $3d$-transition ions as monitors. As these measurements are pursued at our laboratory and elsewhere, it should be possible to determine which impurities are effective in suppressing radiation damage and the mechanism for interstitial trapping.

†Present address: Physics Dept., Pusan National University, Pusan, Korea.

‡Permanent address: Physics Dept., West Virginia University, Morgantown, W. V.
^{1}*Point Defects in Solids*, edited by J. H. Crawford and L. M. Slifkin (Plenum, New York, 1972).

[2]L. W. Hobbs, A. E. Hughes, and D. Pooley, Phys. Rev. Lett. <u>29</u>, 234 (1972); Proc. R. Soc. A <u>332</u>, 167 (1973).

[3]R. H. Silsbee, J. Appl. Phys. <u>28</u>, 1246 (1957).

[4]D. Pooley, Proc. Phys. Soc. <u>87</u>, 245 (1966); <u>87</u>, 257 (1966).

[5]J. H. Crawford, Adv. Phys. <u>17</u>, 93 (1968).

[6]E. Sonder and W. A. Sibley, in Ref. 1.

[7]W. A. Sibley and O. E. Facey, Phys. Rev. <u>174</u>, 1076 (1968).

[8]M. R. Buckton and D. Polley, J. Phys. C 5, 1553 (1972).

[9]W. A. Sibley, S. I. Yun, and W. E. Vehse, J. Phys. C <u>6</u>, 1105 (1973).

[10]L. A. Kappers, S. I. Yun, and W. A. Sibley, Phys. Rev. Lett. <u>29</u>, 943 (1972).

[11]S. I. Yun, L. A. Kappers, and W. A. Sibley, Phys. Rev. B <u>8</u>, 773 (1973).

[12]W. E. Vehse and W. A. Sibley, Phys. Rev. B <u>6</u>, 2443 (1972).

[13]M. N. Kabler, in Ref. 1.

[14]D. Pooley and W. A. Runciman, J. Phys. C <u>3</u>, 1815 (1970).

[15]C. R. Riley and W. A. Sibley, Phys. Rev. B <u>1</u>, 2789 (1970).

[16]J. T. Lewis, J. L. Kolopus, E. Sonder, and M. M. Abraham, Phys. Rev. B <u>7</u>, 810 (1973).

[17]M. Ikeya and N. Itoh, J. Phys. Soc. Japan <u>29</u>, 1295 (1970); J. Phys. Chem. Solids <u>32</u>, 2569 (1971).

[18]C. E. Moore, *Atomic Energy Levels*, Natl. Bur. Stand. Circ. No. 467 (U. S. GPO, Washington, D.C., 1952), Vol. II.

[19]J. Ferguson and H. J. Guggenheim, Phys. Rev. B <u>1</u>, 4223 (1970).